



## **A Low-Complexity Near-Optimal Detector for Multispan Zero-Dispersion Fiber-Optic Channels**

Downloaded from: <https://research.chalmers.se>, 2025-06-18 03:01 UTC

Citation for the original published paper (version of record):

Esmaeili Tavana, M., Keykhosravi, K., Aref, V. et al (2018). A Low-Complexity Near-Optimal Detector for Multispan Zero-Dispersion Fiber-Optic Channels. European Conference on Optical Communication, ECOC, 2018-September. <http://dx.doi.org/10.1109/ECOC.2018.8535237>

N.B. When citing this work, cite the original published paper.

# A Low-Complexity Near-Optimal Detector for Multispan Zero-Dispersion Fiber-Optic Channels

Morteza Tavana<sup>(1)</sup>, Kamran Keykhosravi<sup>(1)</sup>, Vahid Aref<sup>(2)</sup>, Erik Agrell<sup>(1)</sup>

<sup>(1)</sup> Department of Electrical Engineering, Chalmers University of Technology, Gothenburg, Sweden, [tavanam@chalmers.se](mailto:tavanam@chalmers.se)

<sup>(2)</sup> Nokia Bell Labs, Lorenzstr. 10, 70435 Stuttgart, Germany

**Abstract** We design a novel receiver based on the theoretical finding that the linear phase noise is uncorrelated with the nonlinear phase noise. The implementation of the proposed receiver is straightforward and it performs almost equally to the optimal detector at a much lower complexity.

## Introduction

The Kerr nonlinearity results in intra- and inter-channel distortions, whose effects can be mitigated via a variety of techniques<sup>1,2</sup>. In single-channel transmission, the nonlinear phase noise (NLPN) or self-phase modulation is a dominant nonlinear impairment<sup>3–5</sup>. Hence, the quest for efficient methods of compensating the effect of NLPN has spurred a great deal of research. It has been shown that the received signal power can be used to compensate for the NLPN, since these are correlated. Such compensation can be done optically<sup>6</sup> or electronically<sup>7</sup>.

Most previous works on nonlinearity mitigation for zero-dispersion fiber links have assumed ideal distributed amplification, for which the exact Maximum-likelihood (ML) decision regions have been derived<sup>8</sup>. ML detection and optimal decision regions for distributed amplified systems and multilevel PSK modulation were investigated in<sup>8</sup>. For lumped amplification, a learning-based approach was proposed in<sup>9</sup>, however little work has been performed on ML detection in this more practical scenario.

In this paper, we design a suboptimal *per-sample* detector for coherent fiber-optic links, where the NLPN is the dominant system impairment. The per-sample model with zero dispersion has been widely studied before<sup>7,8,10</sup>. We consider long-haul transmission with multiple spans of lumped amplification. We find a low-complexity detector which performs close to the ML detector.

## Channel Model

The most common zero-dispersion model for fiber links with lumped amplification is Mecozzi's model<sup>11,7,5</sup>. The block diagram of this channel is shown in Fig. 1. Here, we consider a fiber-optic link with  $N$  spans of length  $L$  and attenuation coefficient of  $\alpha$ . At the end of each span an optical

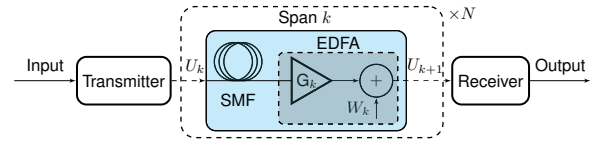


Fig. 1: A lumped amplified fiber-optic link with  $N$  spans.

amplifier (e.g., EDFA) with power gain  $G = e^{\alpha L}$  perfectly compensates for the attenuation of the single mode fiber (SMF)<sup>5</sup>. In Fig. 1, in each span, the input–output relationship is

$$U_{k+1} = U_k \exp(j\gamma L_{\text{eff}} |U_k|^2) + W_k, \quad 1 \leq k \leq N, \quad (1)$$

where  $k$  is the span index,  $U_k$  is the signal samples at the input of the  $k$ th span,  $L_{\text{eff}} = (1 - e^{-\alpha L}) / \alpha$ , and  $W_k \sim \mathcal{CN}(0, 2n_{\text{sp}}(G - 1)h\nu B)$  is the noise added by the  $k$ th amplifier. The parameters are given in Tab. 1. Let  $X \triangleq U_1$ ,  $Y \triangleq U_{N+1}$ , and  $Z_i \triangleq \sum_{k=1}^i W_k \exp(-j\gamma L_{\text{eff}} \sum_{l=1}^k |U_l|^2)$ . The input–output relationship of the overall channel is

$$Y = (X + Z_N) e^{j\Phi_{\text{NLP}}}, \quad (2)$$

where  $\Phi_{\text{NLP}} \triangleq \gamma L_{\text{eff}} \left\{ |X|^2 + \sum_{i=1}^{N-1} |X + Z_i|^2 \right\}$  is the NLPN. The linear phase noise is  $\Phi_L \triangleq \psi(\arg(X + Z_N) - \arg(X))$ , where  $\psi(x) \triangleq (x \bmod 2\pi) - \pi$ , and  $x \bmod 2\pi$  is a modulo operator, which returns the remainder of  $x$  divided by  $2\pi$ .

## Existing Detectors

Here we describe two previously considered detectors: the modified two-stage (MTS) detector, and the back-rotation (BR) detector.

**MTS detector:** The MTS detector is a modified variant of the two-stage detector proposed in<sup>10</sup>. It comprises two successive stages. Let  $x = r \exp(j\phi)$  be the transmitted symbol. First, MAP detection is performed to estimate  $r$  from  $|y|$  and  $\mathcal{X}$ . Let  $\hat{r}$  be the estimation of  $r$ . A phase ro-

**Tab. 1:** System parameters and their descriptions

| Symbol               | Value                   | Meaning               |
|----------------------|-------------------------|-----------------------|
| $n_{\text{sp}}$      | 1.41                    | Emission factor       |
| $h\nu$               | $1.28 \cdot 10^{-19}$ J | Photon energy         |
| $\alpha_{\text{dB}}$ | 0.2 dB/km               | Fiber attenuation     |
| $\gamma$             | $1.27$ (W km) $^{-1}$   | Nonlinear coefficient |
| $B$                  | 32 GHz                  | Noise bandwidth       |

tation is applied to the received sample  $y$ . This phase rotation is calculated based on <sup>7,8</sup> as

$$\phi_{\text{TS}} = \gamma L_{\text{eff}} \frac{(N+1)}{2} \hat{r}^2 + \gamma L_{\text{eff}} \frac{(N-1)}{2} |y|^2. \quad (3)$$

The second stage of the detection is a minimum distance detector  $\hat{x} = \arg \min_{x \in \mathcal{X}} |x - ye^{-j\phi_{\text{TS}}}|$ .

**BR detector:** In this approach, only the deterministic part of the channel is considered<sup>7,6</sup>. The phase shift for the BR scheme is  $\phi_{\text{BR}} = N\gamma L_{\text{eff}} |y|^2$ . This leads to the minimum distance detector  $\hat{x} = \arg \min_{x \in \mathcal{X}} |x - ye^{-j\phi_{\text{BR}}}|$ .

### Proposed Detector

The optimal detector based on the observation of  $Y = y$  is the ML detector

$$\hat{x} = \arg \max_{x \in \mathcal{X}} f_{Y|X}(y|x), \quad (4)$$

where  $f_{Y|X}(\cdot|\cdot)$  is the conditional probability density function (pdf) and  $\mathcal{X}$  is the constellation set. The exact ML decision boundaries are unknown for systems with lumped inline amplifiers. To design the proposed detector, we first require the following theorem whose proof is omitted due to the lack of space

**Theorem 1.** *The linear phase noise  $\Phi_L$  is uncorrelated with both the received power and  $\Phi_{\text{NL}}$ .*

Accordingly, we developed our near-optimal detector outlined in Algorithm 1. The detector is derived based on a Gaussian approximation of the phase statistics and the assumption of independency between the received power  $|y|^2$  and the modified phase  $\tilde{\theta}_x$  for a given  $X = x$ . Steps 2–4 can be precomputed and stored offline before any transmission takes place. Only Steps 5–9 are computed for every received sample  $y$ . The set of modified phases is defined and computed in Step 5. In Step 6, the set of exact pdfs of the received power is computed. In Step 7, the set of approximate pdfs of the modified phases are computed. Finally, in Step 9, by the assumption of independency between the received power and the modified phase, an approximate ML detector is implemented.

### Numerical Results

We evaluate the performance of the proposed detector in simulations using (1) and the parameters in Tab. 1, and we compare the symbol error

### Algorithm 1 Proposed Detector

**Inputs:**  $y$ : received sample;  $\mathcal{X}$ : constellation set;  $N$ : number of spans;  $L$ : length of each span;  $\alpha$ : fiber attenuation;  $\gamma$ : nonlinear coefficient;  $\sigma^2 = n_{\text{sp}}(e^{\alpha L} - 1)h\nu B$ ;  $L_{\text{eff}} = (1 - e^{-\alpha L})/\alpha$ .

**Output:**  $\hat{x}$ : detected symbol.

- 1: **for**  $x \in \mathcal{X}$  **do**
- 2:  $\{\mu_{\theta|x}\} \leftarrow \frac{\gamma L_{\text{eff}}(N+1)(3|x|^4 + (4N-1)\sigma^2|x|^2 + 2N(N-1)\sigma^4)}{6(|x|^2 + N\sigma^2)} + \arg(x)$
- 3:  $\{\sigma_{\theta|x}^2\} \leftarrow \frac{N(N^2-1)(\gamma L_{\text{eff}}\sigma)^2(|x|^4 + 2N\sigma^2|x|^2 + \frac{2N^2+1}{3}\sigma^4)}{3(|x|^2 + N\sigma^2)} + \frac{N\sigma^2}{|x|^2}$
- 4:  $\{\zeta_x\} \leftarrow \frac{-\gamma L_{\text{eff}}(N-1)[|x|^2 + \frac{2N-1}{3}\sigma^2]}{2(|x|^2 + N\sigma^2)}$
- 5:  $\{\tilde{\theta}_x\} \leftarrow \psi(\arg(y) + \zeta_x|y|^2 - \mu_{\theta|x}) + \mu_{\theta|x}$
- 6:  $\{f_{p|x}\} \leftarrow \frac{1}{2N\sigma^2} \exp\left(-\frac{|x|^2 + |y|^2}{2N\sigma^2}\right) I_0\left(\frac{|xy|}{N\sigma^2}\right)$
- 7:  $\{\hat{f}_{\tilde{\theta}|x}\} \leftarrow \frac{1}{\sigma_{\theta|x}\sqrt{2\pi} \operatorname{erf}\left(\frac{\pi}{\sigma_{\theta|x}\sqrt{2}}\right)} \exp\left(-\frac{(\tilde{\theta}_x - \mu_{\theta|x})^2}{2\sigma_{\theta|x}^2}\right)$
- 8: **end for**
- 9:  $\hat{x} \leftarrow \arg \max_{x \in \mathcal{X}} f_{p|x} \hat{f}_{\tilde{\theta}|x}$

rate (SER) of the proposed detector with the BR, MTS, and ML detectors. We consider a single-polarization multi-span zero-dispersion fiber-optic link with a standard square 16-QAM constellation. The transmission system operates at 32 Gbaud corresponding to a data rate of 128 Gbit/s.

For the ML detector, we numerically find the decision regions using a histogram-based pdf estimation for each transmission power. First, we consider two-dimensional grid coordinates for the received sample space. The dimensions are the radius  $|Y|$  and the phase  $\arg(Y)$ . Then, we generate a large number of samples for each 16-QAM symbols. These samples are transmitted through the channel. After that, we locate the received samples in the cells of the defined grid, and we count the number of samples in each cell. Finally, we allocate each cell to the symbol with the highest number of samples in it. Using finer grids and higher number of samples, these decision regions converge to the exact ML decision regions.

To show the effectiveness of the proposed detector, in Fig. 2, we compare the decision regions of the ML detector with the other schemes. We generate  $1.2 \times 10^{12}$  samples for each 16-QAM symbols to draw the ML decision regions. We consider a grid resolution of  $500 \times 500$  for all schemes. In Fig. 2(a), there is an almost perfect match between the ML regions and those of the proposed detector. Fig. 3 represents the SER for various transmission power levels and different

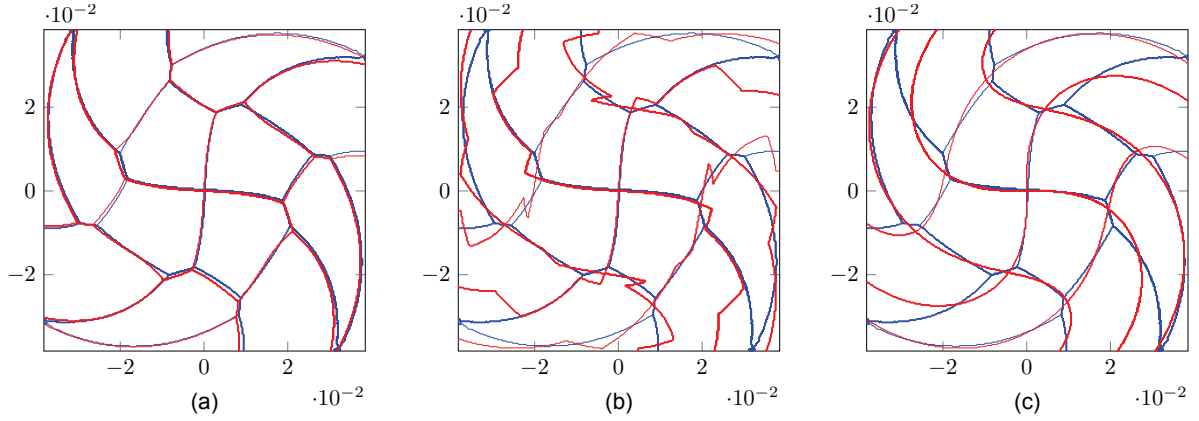


**Fig. 2:** Comparison of 16 decision regions of the ML detector (blue) with the ones of (a) proposed detector, (b) MTS, and (c) BR on a link with  $N = 20$  spans of length  $L = 100$  km at 32 Gbaud with a 16-QAM constellation and  $P_t = 0$  dBm.

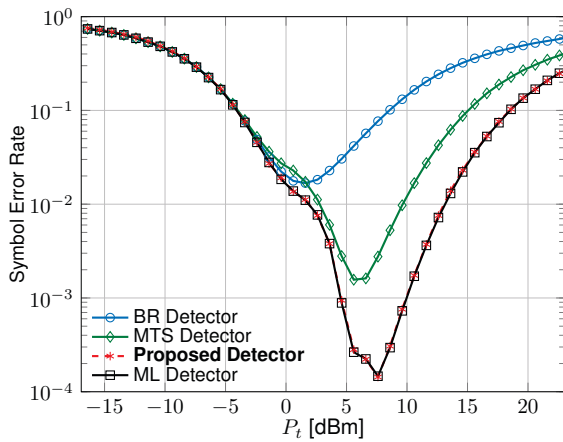


**Fig. 3:** SER of the proposed detector and other schemes.

detectors. It can be seen that the SER of our proposed scheme is very close to that of the ML detector, and it is better than the BR and MTS detectors. In comparison to the proposed detector, the implementation of the ML detector is very complex. The proposed detector achieves the same performance with much lower complexity.

## Conclusions

In this paper, we rigorously showed that the linear phase noise and the NLPN are uncorrelated, which enables the design of a new type of low-complexity detector for zero-dispersion links. Our Monte Carlo simulations indicate that the proposed receiver outperforms state-of-the-art low-complexity detectors, including the MTS and the BR detectors, and its SER is almost equal to that of the ML detector. Derivation of this detector should only be regarded as a first step towards new near-optimal detectors for more realistic long-haul scenarios, including both dispersion and nonlinearity. A natural next step would therefore be to extend these promising results to dispersive fiber links.

## Acknowledgements

This work was supported by the European Commission under grant MSCA-ITN-EID-676448 and the Swedish Research Council under grant 2013-5271. The simulations were carried out on the resources provided by the Swedish National Infrastructure for Computing (SNIC) at C3SE.

## References

- [1] R. Dar, M. Feder, A. Mecozzi, and M. Shttaif, "Inter-channel nonlinear interference noise in WDM systems: Modeling and mitigation," *J. Lightwave Technol.*, Vol. **33**, no. 5, pp. 1044–1053 (2015).
- [2] K. Keykhosravi, M. Tavana, E. Agrell, and G. Durisi, "Demodulation and detection schemes for a memoryless optical WDM channel," to appear in *IEEE Trans. Commun.*, (2018).
- [3] J. P. Gordon and L. F. Mollenauer, "Phase noise in photonic communications systems using linear amplifiers," *Opt. Lett.*, Vol. **15**, no. 23, pp. 1351–1353 (1990).
- [4] G. P. Agrawal, *Nonlinear Fiber Optics*, Academic Press, fourth edition (2006).
- [5] K.-P. Ho, *Phase-Modulated Optical Communication Systems*, Springer (2005).
- [6] X. Liu, X. Wei, R. E. Slusher, and C. J. McKinstrie, "Improving transmission performance in differential phase-shift-keyed systems by use of lumped nonlinear phase-shift compensation," *Opt. Lett.*, Vol. **27**, no. 18, pp. 1616–1618 (2002).
- [7] K.-P. Ho and J. M. Kahn, "Electronic compensation technique to mitigate nonlinear phase noise," *J. Lightwave Technol.*, Vol. **22**, no. 3, pp. 779–783 (2004).
- [8] A. P. Tao Lau and J. M. Kahn, "Signal design and detection in presence of nonlinear phase noise," *J. Lightwave Technol.*, Vol. **25**, no. 10, pp. 3008–3016 (2007).
- [9] A. S. Tan, H. Wymeersch, P. Johannisson, E. Agrell, P. A. Andrekson, and M. Karlsson, "An ML-based detector for optical communication in the presence of nonlinear phase noise," in *IEEE International Conference on Communications (ICC)* (2011).
- [10] C. Häger, A. Graell i Amat, A. Alvarado, and E. Agrell, "Design of APSK constellations for coherent optical channels with nonlinear phase noise," *IEEE Trans. Commun.*, Vol. **61**, no. 8, pp. 3362–3373 (2013).
- [11] A. Mecozzi, "Limits to long-haul coherent transmission set by the Kerr nonlinearity and noise of the in-line amplifiers," *J. Lightwave Technol.*, Vol. **12**, no. 11, pp. 1993–2000 (1994).